

Inhibition of Corrosion of Carbon Steel in 0.5 M HCl Solutions by Some Pyridopyrimidine Derivatives

A.S. Fouda^{*a}, M. Diab^b, A. El-Bindary^b, A. Bakr^a

^a *Department of Chemistry, Faculty of Science, Mansoura University, Egypt*

^b *Department of Chemistry, Faculty of Science, Damietta University, Egypt*

*Corresponding author (Tel: +20.50.2365730; Fax: +20.50.2246254, email: asfouda@mans.edu.eg)

Abstract

The influence of some Pyridopyrimidine derivatives on the corrosion of carbon steel in 0.5 M HCl was investigated using weight loss, potentiodynamic polarization, electrochemical impedance spectroscopy (EIS) and electrochemical frequency modulation (EFM) techniques. The inhibition efficiency increases with increasing the inhibitor concentration, but decreases with increasing the temperature. The inhibitors were adsorbed on the carbon steel surface following Temkin's adsorption isotherm. The electrochemical results indicated that all the investigated compounds act as mixed-type inhibitors. Some thermodynamic parameters for corrosion and adsorption processes were determined and discussed. The mechanism of inhibition process was discussed in the light of the chemical structure and quantum-chemical calculations of the investigated inhibitors.

Keywords: corrosion inhibition; carbon steel; EIS; EFM; HCl; pyridopyrimidine derivative.

Introduction

Corrosion is a fundamental process playing an important role in economics and safety, particularly for metals. The use of inhibitors is one of the most practical methods for protection against corrosion, especially in acidic media [1]. Most well-known acid inhibitor is organic compounds containing nitrogen, sulfur, and oxygen atoms. Among them, organic inhibitors have many advantages such as high inhibition efficiency, low price, low toxicity, and easy production [2-5]. Organic heterocyclic compounds have been used for the corrosion inhibition of iron [6-11], copper [12], aluminum [13-15], and other metals [16-17] in different corroding media. The adsorption of the surfactant heterocyclic compounds on the metal surface can markedly change the corrosion-resisting property of the metal [18-19] and so the study of the

relations between the adsorption and corrosion inhibition is of great importance. Heterocyclic compounds have shown a high inhibition efficiency for iron in both HCl [20] and H₂SO₄ [21] solutions.

As pyridopyrimidine derivatives have rarely been studied as inhibitors for C-steel in HCl. For this reason, the objective of the present work is to investigate the inhibiting action of Pyridopyrimidine derivatives in 0.5M HCl at 25-55 °C using different methods.

Materials and methods

Materials preparation

Tests were performed on C-steel specimens of the following composition (weight %): 0.200 % C, 0.350 % Mn, 0.024 % P, 0.003 % S, and the remainder Fe.

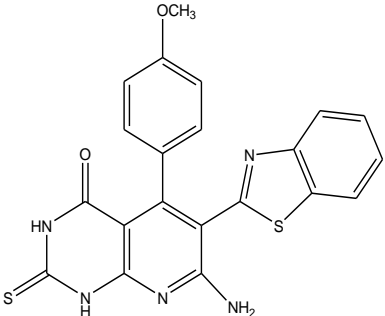
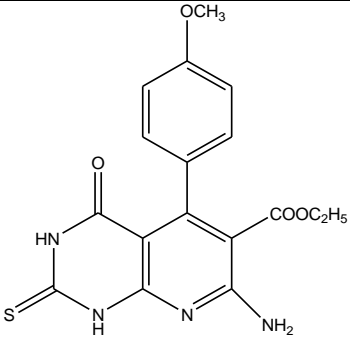
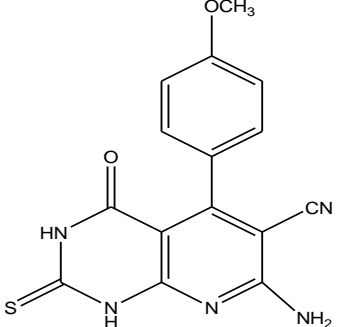
Solutions

The aggressive solution, 0.5 M HCl was prepared by dilution of analytical grade (37 %) HCl with bi-distilled water. The concentration range of the inhibitors used was 1×10^{-6} - 21×10^{-6} M.

Inhibitors

The investigated compounds were selected from Pyridopyrimidine derivatives and are shown in table (1).

Table 1 The molecular structure of investigated inhibitors

Inh.	Structure	IUPAC Name	Mol. Wt.	Active center	Chemical formula
(A)		7-amino-6-(benzo[d]thiazol-2-yl)-2,3-dihydro[2,3-d]pyrimidin-4(1H)-one	433.51	2O 5N 2S	$C_{21}H_{15}N_5O_2S_2$
(B)		Ethyl 7-amino-1,2,3,4-tetrahydro-5-(4-methoxyphenyl)-4-oxo-2-thioxopyrido[2,3-d]pyrimidine-6-carboxylate	372.4	4O 4N 1S	$C_{17}H_{16}N_4O_4S$
(C)		7-amino-1,2,3,4-tetrahydro-5-(4-methoxyphenyl)-4-oxo-2-thioxopyrido[2,3-d]pyrimidine-6-carbonitrile	325.35	2O 5N 1S	$C_{15}H_{11}N_5O_2S$

Weight loss measurements

Seven parallel carbon steel sheets of $25 \times 20 \times 0.6$ mm were abraded with emery paper (grade 320–500–800) and then washed with bidistilled water and acetone. After accurate weighing, the specimens were immersed in a 250 ml beaker, which contained 250 ml of HCl with and without addition of different concentrations of investigated inhibitors.

All the aggressive acid solutions were open to air. After 3 h, the specimens were taken out, washed, dried, and weighed accurately. The average weight loss of seven parallel C-steel sheets could be obtained. The inhibition efficiency (IE %) and the degree of surface coverage, θ , of Pyridopyrimidine derivatives for the corrosion of C-steel were calculated as follows [22],

$$IE\% = \theta \times 100 = [1 - (W/W^0)] \times 100 \quad (1)$$

where W° and W are the average weight losses without and with addition of the inhibitor, respectively.

Electrochemical measurements

Polarization experiments were carried out in a conventional three-electrode cell with a platinum counter electrode and a saturated calomel electrode (SCE) coupled to a fine Luggin capillary as reference electrode. The working electrode was in the form of a square cut from C-steel sheet embedded in epoxy resin of polytetrafluoroethylene (PTFE) so that the flat surface was the only surface of the electrode. The working surface area was 1 cm^2 . Tafel polarization curves were obtained by changing the electrode potential automatically from -500 to +500 mV at open circuit potential with a scan rate of 1 mVs^{-1} . Stern-Geary method [23] used for the determination of corrosion current is performed by extrapolation of anodic and cathodic Tafel lines to a point which gives $\log i_{\text{corr}}$ and the corresponding corrosion potential (E_{corr}) for inhibitor free acid and for each concentration of inhibitor. Then i_{corr} was used for calculation of inhibition efficiency and surface coverage (θ) as below:

$$\text{IE \%} = \theta \times 100 = [1 - (i_{\text{corr(inh)}} / i_{\text{corr(free)}})] \times 100 \quad (2)$$

Where $i_{\text{corr(free)}}$ and $i_{\text{corr(inh)}}$ are the corrosion current densities in the absence and presence of inhibitor, respectively.

Impedance measurements were carried out in frequency range from 100 kHz to 10 mHz with amplitude of 5 mV peak-to-peak using ac signals at open circuit potential. The experimental impedance were analyzed and interpreted on the basis of the equivalent circuit. The main parameters deduced from the analysis of Nyquist diagram are the resistance of charge transfer R_{ct} (diameter of high frequency loop) and the capacity of double layer C_{dl} which is defined as:

$$C_{\text{dl}} = 1 / (2 \pi f_{\text{max}} R_{\text{ct}}) \quad (3)$$

where f_{max} is the maximum frequency.

The inhibition efficiencies and the surface coverage (θ) obtained from the impedance measurements were defined by the following relation:

$$\text{IE \%} = \theta \times 100 = [1 - (R_{\text{ct}}^{\circ} / R_{\text{ct}})] \times 100 \quad (4)$$

where R_{ct}° and R_{ct} are the charge transfer resistance in the absence and presence of inhibitor, respectively.

The electrode potential was allowed to stabilize 30 min before starting the measurements. All the experiments were

conducted at $25 \pm 1^{\circ}\text{C}$. Measurements were performed using Gamry (PCI 300/4) Instrument Potentiostat/Galvanostat/ZRA. This software includes a Gamry framework system based on the ESA 400. Gamry applications include DC105 for corrosion measurements, EIS300 software for electrochemical impedance spectroscopy and EFM140 software for electrochemical frequency modulation along with a computer for collecting data. Echem Analyst 5.58 software was used for plotting, graphing, and fitting data.

Results and Discussion

Weight loss measurements

The weight loss-time curves of C-steel with the addition of inhibitor (A) in 0.5M HCl at various concentrations is shown in Fig. 1. Similar curves were obtained in presence of the other inhibitors, but not shown. The curves of Fig. 1 show that the weight loss values of C-steel in 0.5M HCl solution containing investigated inhibitor decrease as the concentration of the inhibitor increases; i.e., the corrosion inhibition strengthens with the inhibitor concentration, this is appear in the Table 2. This trend may result from the fact that the adsorption of inhibitor on the C-steel increases with the inhibitor concentration thus the C-steel surface is efficiently separated from the medium by the formation of a film on its surface [24-25]. The inhibition efficiency of investigated compounds in the order : $A > B > C$.

Potentiodynamic polarization measurements

Fig. 2 shows the anodic and cathodic Tafel polarization curves for C-steel in 0.5 M HCl in the absence and presence of varying concentrations of inhibitor A at 25°C . Similar curves were obtained in presence of the other inhibitors, but not shown. From Fig. 2, it is clear that both anodic metal dissolution and cathodic H_2 reduction reactions were inhibited when investigated inhibitors were added to 0.5 M HCl and this inhibition was more pronounced with increasing inhibitor concentration. Tafel lines are shifted to more negative and more positive potentials with respect to the blank curve by increasing the concentration of the investigated inhibitors. This behavior indicates that the undertaken additives act as mixed-type inhibitors [25-26]. The results show that the increase in

inhibitor concentration leads to decrease the corrosion current density (i_{corr}), but the Tafel slopes (β_a , β_c), are approximately constant indicating that the retardation of the two reactions (cathodic hydrogen reduction and anodic metal dissolution) were affected without changing the dissolution mechanism [27-29]. The order of inhibition efficiency of investigated compounds in the order: $A > B > C$.

Table 2 Variation of IE % of different compounds with their molar concentrations at 25°C from weight loss measurements at 120 min immersion in 0.5 M HCl

Comp	Conc $\times 10^{-6}$ M	Weight loss, mg cm^{-2}	Corrosion Rate (CR) mg cm^{-2} min^{-1} mg cm^{-2} min^{-1}	IE %
Blank	0.0	2.80	0.023	-
A	1	2.10	0.018	25.00
	5	1.70	0.014	39.30
	9	0.90	0.008	67.86
	17	0.50	0.004	82.14
	21	0.20	0.001	92.86
B	1	4.80	0.040	20.80
	5	3.80	0.032	35.40
	9	2.40	0.020	50.00
	17	1.80	0.015	62.50
	21	0.07	0.001	85.42
C	1	4.40	0.037	15.90
	5	3.70	0.031	25.00
	9	3.30	0.028	38.60
	17	2.70	0.023	59.10
	21	1.10	0.009	75.00

Electrochemical impedance spectroscopy (EIS)

The effect of inhibitor concentration on the impedance behavior of carbon steel in 0.5M HCl solution at 25 °C is presented in Fig. 3 (a, b). The curves show a similar type of Nyquist plots for C-steel in the presence of various concentrations of inhibitor (A), similar curves were obtained for other inhibitors but not shown. The existence of single semi-circle showed the single charge transfer process during dissolution which is unaffected by the presence of inhibitor molecules. Deviations from perfect circular shape are often referred to the frequency dispersion of interfacial impedance which arises due to surface roughness, impurities, dislocations, grain boundaries, adsorption of inhibitors, and formation of porous layers and in homogenates of

the electrode surface [30-31]. Inspections of the data reveal that each impedance diagram consists of a large capacitive loop with one capacitive time constant in the Bode-phase plots (Fig.3b). The electrical equivalent circuit model is shown in Fig. 4. It used to analyze the obtained impedance data. The model consists of the solution resistance (R_s), the charge-transfer resistance of the interfacial corrosion reaction (R_{ct}) and the double layer capacitance (C_{dl}). Excellent fit with this model was obtained with our experimental data. EIS data (Table 3) show that the R_{ct} values increases and the C_{dl} values decreases with increasing the inhibitor concentrations. This is due to the gradual replacement of water molecules by the adsorption of the inhibitor molecules on the metal surface, decreasing the extent of dissolution reaction. The higher (R_{ct}) values, are generally associated with slower corroding system [32-33].

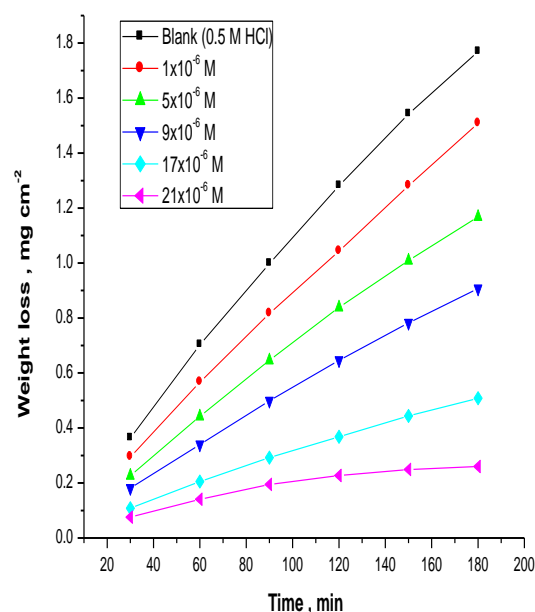


Fig. 1 Weight loss-time curves for the corrosion of carbon steel in 0.5 M HCl in the absence and presence of different concentrations of inhibitor (A) at 25 °C

The decrease in the C_{dl} can result from the decrease of the local dielectric constant and/or from the increase of thickness of the electrical double layer suggested that the inhibitor molecules function by adsorption at the metal/solution interface [34]. The IE% obtained from EIS measurements are close to those deduced from polarization measurements. The order of inhibition efficiency obtained from EIS measurements is as follows: $A > B > C$.

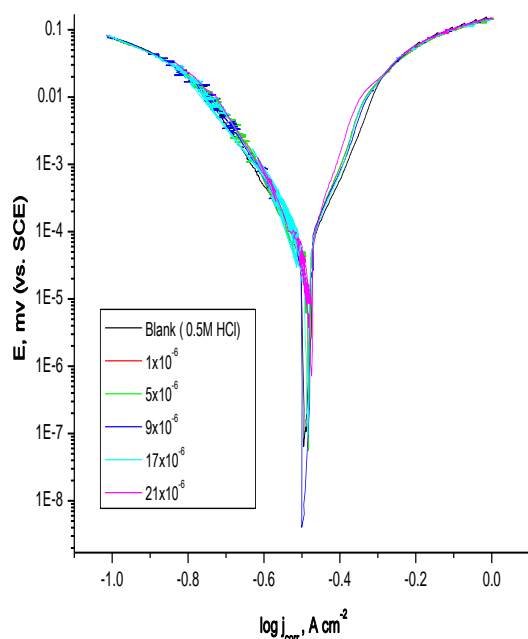


Fig. 2 Potentiodynamic polarization curves for corrosion of C-steel in 0.5 M HCl in the absence and presence of different concentrations of inhibitor (A) at 25 °C

Table 3 EIS data of C-steel in 0.5 M HCl and in the absence and presence of different concentrations of investigated inhibitors at 25 °C

Comp.	Conc., M	$C_{dl}, \times 10^{-3} \mu Fc m^{-2}$	$R_{CT}, \times 10^{-4} \Omega cm^2$	θ	IE%
Blank	Blank	2.87	34.90	---	---
Inhibitor A	1×10^{-6}	2.12	49.86	0.301	30.1
	5×10^{-6}	1.83	68.43	0.490	49.0
	9×10^{-6}	1.51	96.94	0.636	63.6
	17×10^{-6}	1.36	166.19	0.791	79.1
	21×10^{-6}	1.11	317.27	0.897	89.7
Inhibitor B	1×10^{-6}	2.42	49.15	0.293	29.3
	5×10^{-6}	1.91	58.17	0.401	40.1
	9×10^{-6}	1.70	74.26	0.525	52.5
	17×10^{-6}	1.33	112.58	0.691	69.1
	21×10^{-6}	1.21	205.29	0.829	82.9
Inhibitor C	1×10^{-6}	2.33	39.21	0.112	11.2
	5×10^{-6}	2.06	46.53	0.249	24.9
	9×10^{-6}	1.31	54.53	0.365	36.5
	17×10^{-6}	0.98	81.16	0.571	57.1
	21×10^{-6}	0.88	129.26	0.732	73.2

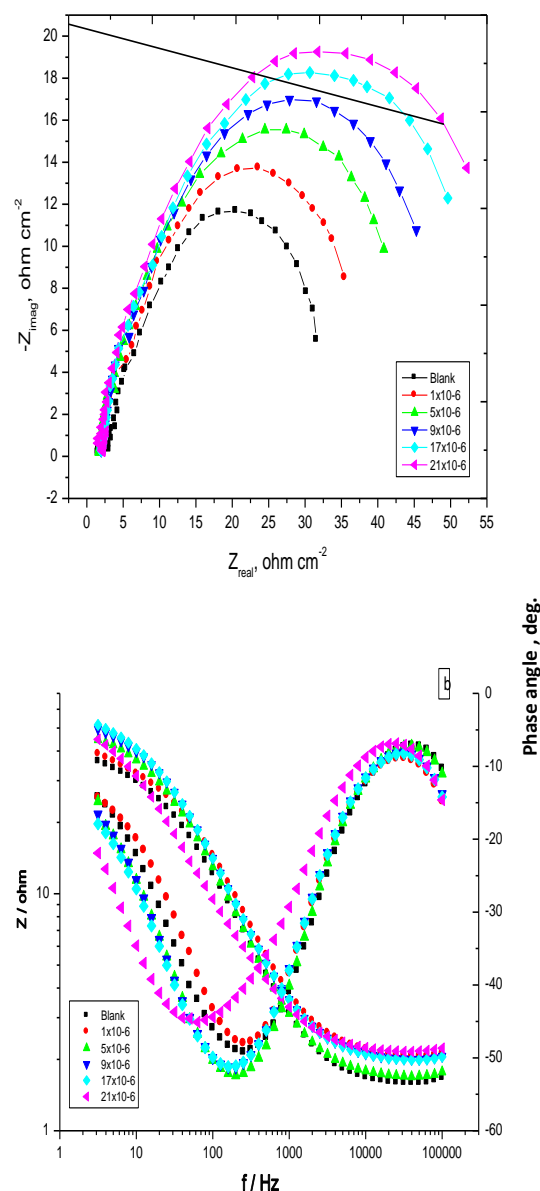


Fig. 3 The Nyquist (a) and Bode (b) plots for corrosion of C-steel in 0.5 M HCl in the absence and presence of different concentrations of compound (1) at 25 °C

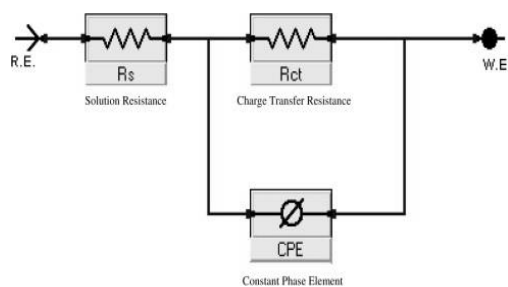


Fig. 4 Electrical equivalent circuit model used to fit the results of impedance

Electrochemical frequency modulation (EFM) measurements

Electrochemical frequency modulation is a non destructive corrosion measurement technique that can directly give values of the corrosion current without prior knowledge of Tafel constants. Like EIS, it is a small signal AC technique. Unlike EIS, however, two sine waves (at different frequencies) are applied to the cell simultaneously.

The results of EFM experiments are a spectrum of current response as a function of frequency. The spectrum is called the intermodulation spectrum. The spectra contain current responses assigned for harmonical and intermodulation current peaks. The corrosion rate and Tafel parameters can be obtained with one measurement by analyzing the harmonic frequencies. The larger peaks were used to calculate the corrosion current density (i_{corr}), the

Tafel slopes (β_c and β_a) and the causality factors (CF-2 and CF-3). Intermodulation spectra obtained from EFM measurements. As can be seen from Table (3), Then i_{corr} was subsequently obtained and used for calculation of inhibition efficiency (IE %) and degree of surface coverage (θ) were calculated from the following equation:

$$\text{IE \%} = [1 - (i_{\text{corr (inh)}} / i_{\text{corr (free)}})] \times 100 = \theta \quad (5)$$

where $i_{\text{corr (free)}}$ and $i_{\text{corr (inh)}}$ is the corrosion current in absence and presence of inhibitors, respectively.

The causality factors in Table (4) are very close to theoretical values according to the EFM theory [34].

The order of the inhibition efficiency obtained is as follows: A > B > C.

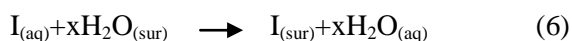
EFM spectra for carbon steel in 0.5 M HCl in the absence and presence of different concentrations from inhibitor (A) (Fig. 5-9). Similar curves were obtained in presence of the other inhibitors, but not shown.

Table 4 Electrochemical kinetic parameters obtained by EFM technique for carbon steel in the absence and presence of various concentrations of inhibitors in 0.5 M HCl at 25 °C

Comp	Conc., $\times 10^{-6}$ M	I_{corr} μAcm^{-2}	β_c mVdec^{-1}	β_a mVdec^{-1}	CF-2	CF-3	CR mpy	θ	IE%
Blank	0.0	1952.0	350.6	579.0	1.97	2.99	892	-	-
A	5	1061.9	239.2	318.2	2.04	6.69	485.3	0.386	38.6
	9	589.5	189.8	416.7	1.97	3.29	269.4	0.579	57.9
	17	294.8	252.2	329.7	2.07	6.65	134.7	0.779	77.9
	21	173.7	191.6	292.9	2.01	1.93	79.4	0.903	90.3
B	5	1169.3	243.7	326.6	2.04	6.09	534.3	0.204	20.4
	9	950.6	225.7	282.8	2.03	7.53	434.4	0.500	50.0
	17	694.9	228.0	302.5	2.04	10.18	317.6	0.720	72.0
	21	271.3	175.1	206.8	1.90	4.22	124.0	0.896	89.6
C	5	1368.4	291.0	401.7	2.02	6.37	625.3	0.119	11.9
	9	1180.9	111.2	136.7	1.53	1.05	539.7	0.361	36.1
	17	759.3	52.1	70.07	1.48	1.75	346.9	0.479	47.9
	21	443.1	47.2	58.53	1.12	1.53	202.5	0.715	71.5

Adsorption isotherm

Organic molecules inhibit the corrosion process by the adsorption on metal surface. Theoretically, the adsorption process can be regarded as a single substitutional process in which an inhibitor molecule, I, in the aqueous phase substitutes an "x" adsorbed on the metal surface [35-36] vis,



where x is known as the size ratio and simply equals the number of adsorbed water molecules

replaced by a single inhibitor molecule. The adsorption depends on the structure of the inhibitor, the type of the metal and the nature of its surface, the nature of the corrosion medium and its pH value, the temperature and the electrochemical potential of the metal-solution interface. Also, the adsorption provides information about the interaction among the adsorbed molecules themselves as well as their interaction with the metal surface.

The values of surface coverage, θ , for different concentration of the studied compound at different temperatures have been used to

explain the best isotherm to determine the adsorption process.

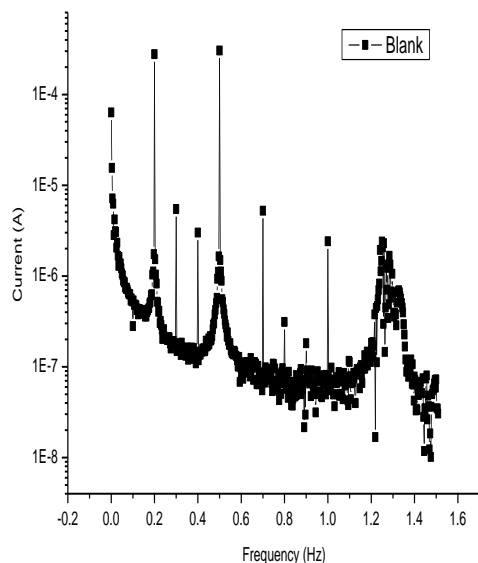


Fig. 5 EFM spectra for carbon steel in 0.5 M HCl (blank)

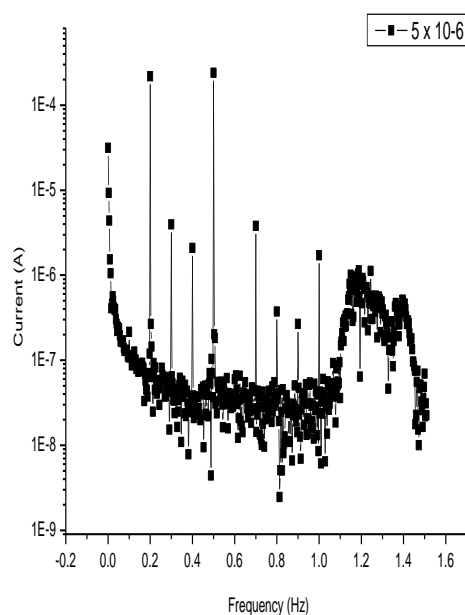


Fig. 6 EFM spectra for carbon steel in 0.5 M HCl in the presence of 5×10^{-6} M from inhibitor (A)

By far the results of investigated inhibitors were best fitted by Temkin adsorption isotherm. Fig. 10 shows the plotting of θ against $\log C$ at 25°C for investigated inhibitors. These plots gave straight lines indicating that the adsorption of investigated compounds on C-steel surface follows Temkin adsorption isotherm: [35].

$$\theta = (1/f) \ln K_{\text{ads}} C \quad (7)$$

where C is the concentration of inhibitor, θ the fractional surface coverage and K_{ads} is the adsorption equilibrium constant related to the free energy of adsorption ΔG_{ads} as [36]:

$$K_{\text{ads}} = 1/55.5 \exp (-\Delta G_{\text{ads}}/RT) \quad (8)$$

where R is the universal gas constant, T is the absolute temperature. The value 55.5 is the concentration of water on the metal surface in mol/l.

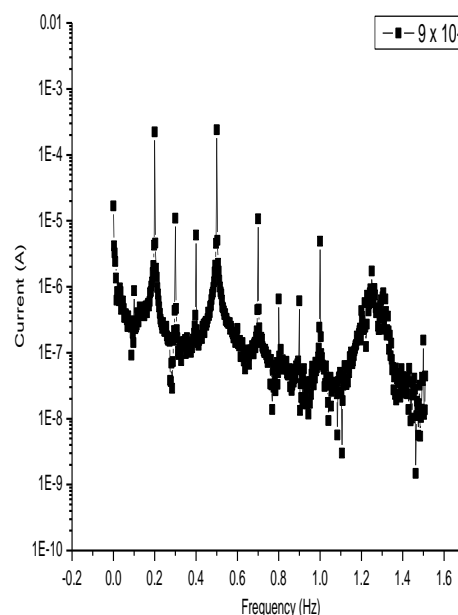


Fig. 7 EFM spectra for carbon steel in 0.5 M HCl in the presence of 9×10^{-6} M from inhibitor (A)

The value of K_{ads} and $\Delta G^{\circ}_{\text{ads}}$ for Pyridoprimumine derivatives were calculated and are recorded in Table (5).

All estimated thermodynamic adsorption parameters for the studied compounds on carbon steel from 0.5 M HCl solution were listed in Tables (5). Inspection of the obtained data, it was found that:

the presence of 21×10^{-6} M inhibitor (A)

- The negative values of $\Delta G^{\circ}_{\text{ads}}$ reflect that the adsorption of studied compounds on C- steel surface from 0.5 M HCl solution is spontaneous process [37-38].
- $\Delta G^{\circ}_{\text{ads}}$ values increase (become less negative) with an increase of temperature which indicates the occurrence of exothermic process at which adsorption was unfavorable with increasing reaction temperature as the

result of the inhibitor desorption from the steel surface [38].

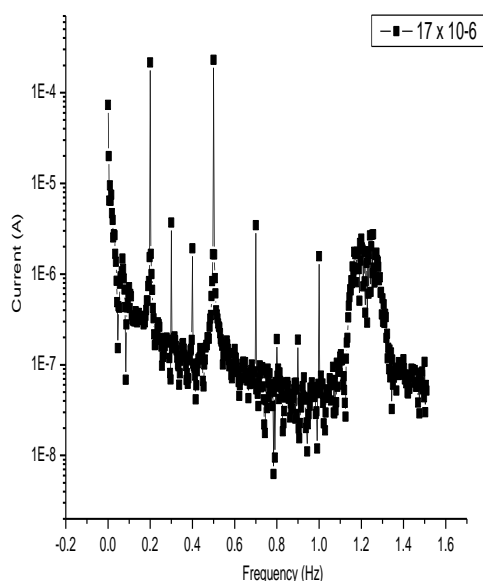


Fig. 8 EFM spectra for carbon steel in 0.5 M HCl in the presence of 17×10^{-6} M from inhibitor (A)

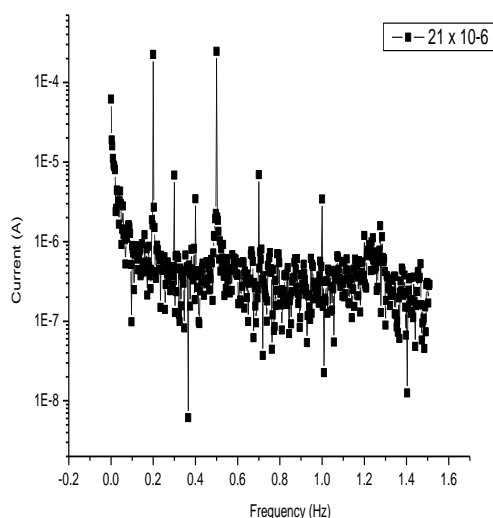


Fig. 9 EFM spectra for carbon steel in 0.5 M HCl in the presence of 21×10^{-6} M inhibitor (A)

Effect of temperature

The effect of temperature on the rate of corrosion of C-steel in 0.5 M HCl containing different concentrations from investigated inhibitors was tested by weight loss method over a temperature range from 25 to 55 °C.

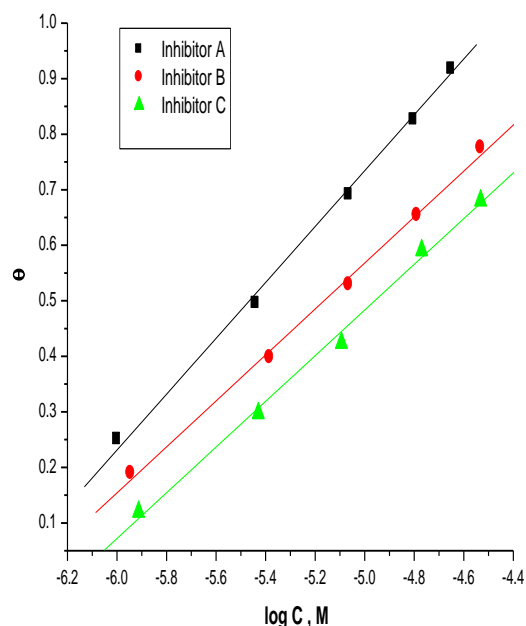


Fig. 10 Temkin adsorption isotherm for investigated inhibitors for corrosion of C-steel in 0.5 M HCl at 25°C

The results revealed that, the rate of corrosion increases as the temperature increases and decreases as the concentration of these compounds increases for all compound used. The activation energy (E_a^*) of the corrosion process was calculated using Arrhenius equation:

$$K = A \exp(-E_a^*/RT) \quad (9)$$

where k is the rate of corrosion, A is the Arrhenius constant, R is the gas constant and T is the absolute temperature.

Fig. 11 presents the Arrhenius plot in the presence and absence of compound (A). Similar curves are obtained in presence of the other inhibitors, but not shown. E_a^* values determined from the slopes of these lines are shown in Table 6. The linear regression (R^2) is close to 1 which indicates that the corrosion of C-steel in 0.5M HCl solution can be elucidated using the kinetic model. Table 6 showed that the value of E_a^* for inhibited solution is higher than that for uninhibited solution, suggesting that dissolution of C-steel is slow in the presence of inhibitor and can be interpreted as due to physical adsorption[39]. It is known from Eq. 8 that the higher E_a^* values lead to the lower corrosion rate. This is due to the formation of a film on the C-steel surface serving as an energy barrier for the C-steel corrosion [40].

Enthalpy and entropy of activation (ΔH^* , ΔS^*) of the corrosion process were calculated from the transition state theory (Table 6):

Rate = $(RT/Nh) \exp(\Delta S^*/R) \exp(-\Delta H^*/RT)$ (10)
where h is Planck's constant and N is Avogadro's number.

Table 5 Thermodynamic parameters for the adsorption of inhibitors on C-steel surface in 0.5 M HCl at different temperatures

Inhib	Temp. °C	$K_{ads} \times 10^{-6}$ M^{-1}	$-\Delta G_{ads}^{\circ}$ $kJ\ mol^{-1}$	$-\Delta H_{ads}^{\circ}$ $kJ\ mol^{-1}$	$-\Delta S_{ads}^{\circ}$ $J\ mol^{-1}\ K^{-1}$
(A)	25	2.22	46.2	79.03	4.748
	35	3.33	46.7		
	45	2.29	49.3		
	55	4.159	52.5		
(B)	2.17	2.17	46.1	23.81	5.941
	2.33	2.33	47.8		
	2.16	2.16	49.7		
	2.44	2.44	51.1		
(C)	1.55	45.3	1.55	79.25	4.779
	3.35	48.8	3.35		
	3.34	49.5	3.34		
	2.88	51.5	2.88		

Table 6 Activation parameters of the corrosion of C-steel in 0.5 M HCl at 21×10^{-6} M for the investigated compounds

Inhibitor	E_a^* , $kJ\ mol^{-1}$	ΔH^* , $kJ\ mol^{-1}$	$-\Delta S^*$, $J\ mol^{-1}\ K^{-1}$
0.5 M HCl	22.42	20.49	185.34-
Inhibitor A	63.57	59.55	-73.91
Inhibitor B	37.53	35.04	-149.02
Inhibitor C	32.93	30.83	-157.96

A plot of $\log(\text{Rate}/T)$ vs. $1/T$ for C-steel in 0.5M HCl at different concentrations from investigated compounds, gives straight lines as shown in Fig. 12 for compound (A). Similar curves were obtained in presence of the other inhibitors, but not shown. The positive signs of ΔH^* reflect the endothermic nature of the steel dissolution process. Large and negative values of ΔS^* imply that the activated complex in the rate-determining step represents an association rather than dissociation step, meaning that decrease in disordering takes place on going from reactants to the activated complex[41-42]. The order of the inhibition efficiencies of Pyridoprimumine

derivatives as gathered from the increase in E_a^* and ΔH^* values and decrease in ΔS^* values is as follows: $A > B > C$.

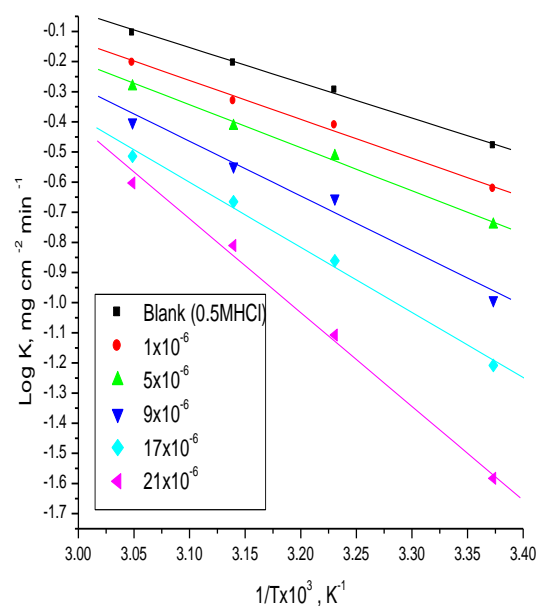


Fig. 11 Log k – $1/T$ curves for C-steel dissolution in 0.5 M HCl in the absence and presence of compound (A)

Quantum chemical parameters of investigated compounds

The E_{HOMO} indicates the ability of the molecule to donate electrons to an appropriated acceptor with empty molecular orbitals but E_{LUMO} indicates its ability to accept electrons. The lower the value of E_{LUMO} , the more ability of the molecule is to accept electrons [43]. While, the higher is the value of E_{HOMO} of the inhibitor, the easier is its offering electrons to the unoccupied d-orbital of metal surface and the greater is its inhibition efficiency. The calculations listed in Table 7 showed that the highest energy E_{HOMO} is assigned for the compound A, which is expected to have the highest corrosion inhibition among the investigated compounds.

Table 7 E_{HOMO} , E_{LUMO} , their energy gap (ΔE_{gap}) and dipole moment (μ) for the different compounds as obtained B3LYP/6-31G(d) method in gas phase

Comp	$-E_{HOMO}$	$-E_{LUMO}$	ΔE_{gap}	μ (Debye)	Area (\AA^2)
A	8.99	1.52	7.47	8.46	400.29
B	9.24	1.62	7.52	4.1	352.09
C	9.29	1.72	7.57	3.75	306.19

The HOMO–LUMO energy gap, ΔE approach, which is an important stability index, is applied to develop theoretical models for explaining the structure and conformation barriers in many molecular systems. The smaller is the value of ΔE , the more is the probable inhibition efficiency that the compound has [44–45]. The dipole moment μ , electric field, was used to discuss and rationalize the structure. It was shown from (Table 7) that compound A molecule has the smallest HOMO–LUMO gap compared with the other molecules. Accordingly, it could be expected that compound (A) molecule has more inclination to adsorb on the metal surface than the other molecules. The higher is the value of μ , the more is the probable inhibition efficiency that the compound has. The calculations showed that the highest value of μ is assigned for the compound A which has the highest inhibition efficiency. Absolute hardness and softness σ are important properties to measure the molecular stability and reactivity. A hard molecule has a large energy gap and a soft molecule has a small energy gap. Soft molecules are more reactive than hard ones because they could easily offer electrons to an acceptor. For the simplest transfer of electrons, adsorption could occur at the part of the molecule where σ , which is a local property, has the highest value. In a corrosion system, the inhibitor acts as a Lewis base while the metal acts as a Lewis acid. Bulk metals are soft acids and thus soft base inhibitors are most effective for acidic corrosion of those metals.

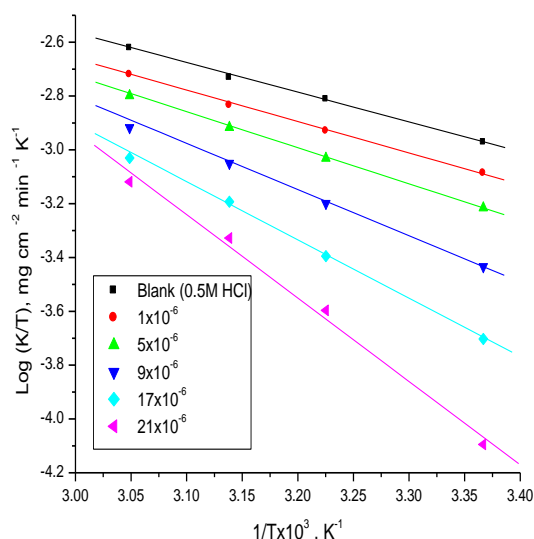


Fig. 12 $\log k/T - 1/T$ curves for C-steel dissolution in 0.5M HCl in the absence and presence of different concentrations the investigated compound (A)

Accordingly, it is concluded that inhibitor with the highest σ value has the highest inhibition

efficiency Table 7 which is in a good agreement with the experimental data. This is also confirmed from the calculated inhibition efficiencies of molecules as a function of the inhibitor chemical potential, P_i , and the fraction of charge transfer, ΔN to the metal surface. The relatively good agreement of P_i and ΔN with the inhibition efficiency could be related to the fact that any factor causing an increase in chemical potential would enhance the electronic releasing power of inhibitor molecule Table 7.

Analysis to estimate the adsorption centers of inhibitors has been widely reported and it is mostly used for the calculation of the charge distribution over the whole skeleton of the molecule. There is a general consensus by several authors that the more negatively charged heteroatom is, the more is its ability to adsorb on the metal surface through a donor–acceptor type reaction. Variation in the inhibition efficiency of the inhibitors depends on the presence of electro negative O- and N-atoms as substituents in their molecular structure. The calculated Mulliken charges of selected atoms are presented in Fig. 13.

Mechanism of Inhibition

Corrosion inhibition of carbon steel in HCl solution by the investigated pyridopyrimidine derivatives indicated from weight loss, potentiodynamic polarization, EIS and EFM techniques was found to depend on the concentration and the nature of the inhibitor. It is generally, assumed that the adsorption of the inhibitors at the metal / solution interface is the first step in the action mechanism of the inhibitors in aggressive acid media.

Four types of adsorption may take place during inhibition involving organic molecules at the metal / solution interface: Electrostatic attraction between charged molecules and charged metal, Interaction of unshared electrons pairs in the molecule with the metal, Interaction of π electrons with the metal, A combination of the above [46]. Concerning inhibitors, the inhibition efficiency depends on several factors; such as number of adsorption sites and their charge densities, molecular size, heat of hydrogenation, mode of interaction with the metal surface, and the formation metallic complexes [47]. Most organic inhibitors contain at least one polar group with an atom of nitrogen, sulfur or oxygen, each of them in principle representing a chemisorptions center. The inhibitive properties of such compounds depend

on the electron densities surrounding the active center where the higher the electron density at the center the more the effective the inhibitor.

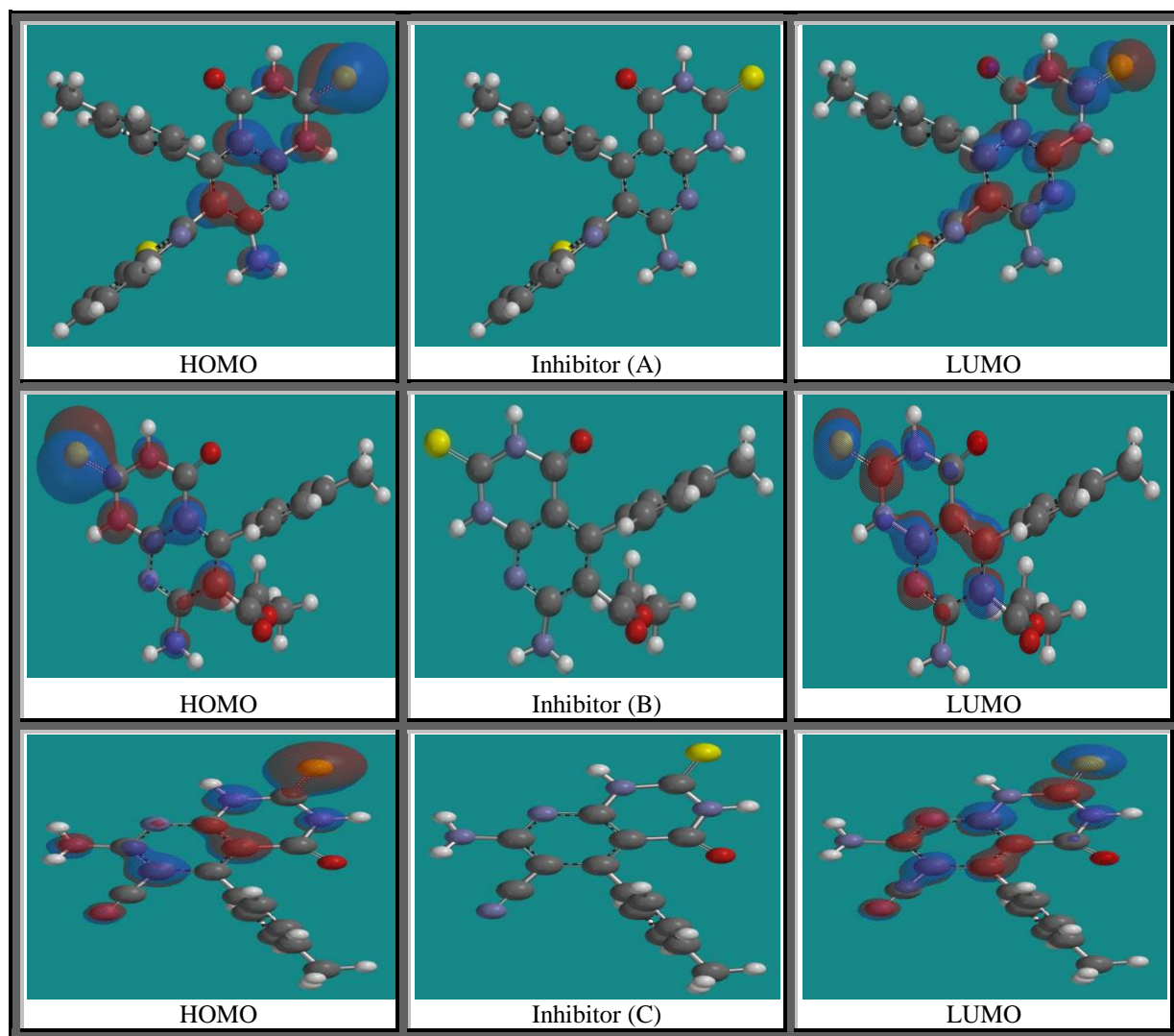


Fig. 13 Optimized molecular structure of inhibitors, and its frontier molecular orbital density distribution (HOMO and LUMO)

In aqueous acidic solutions, the investigated pyridopyrimidine derivatives proposed to exist either as neutral molecules or in the form of cationic (protonated). In general two modes of adsorption could be considered. The neutral form may adsorb on the metal surface by chemisorption's mechanism, involving the displacement of water molecules from the metal surface and the sharing electrons between the N and O atoms and metal surface. On the other hand, it is well known that carbon steel surface has positive charge [48] in acidic solution; therefore it is difficult for protonated inhibitors to adsorb on the positively charged carbon steel surface due to electrostatic repulsion.

Since chloride ions have a smaller degree of hydration being specifically adsorbed, they create an excess negative charge toward the solution and favour more adsorption of the protonated inhibitor. In other words, there may be a synergism between Cl^- and the inhibitor, which improves the inhibitive capability of the inhibitor. When the protonated inhibitor is adsorbed on the metal surface the formation of a coordinate bond due to the partial transfer of electron from S, N- and/or O-atoms to the metal surface may be happened and both anodic and cathodic reactive sites on the steel surface may be blocked and inhibition of both reactions occurred. It is known that compounds differing in the functional donor atom (other factors being equal),

the order of corrosion inhibition is usually: $S > N > O$.

The order of increased inhibition efficiency for pyridopyrimidine derivatives is: $A > B > C$. as indicated from the different methods. Compound (A) is the most efficient inhibitor due to: (i) the presence of two S-atoms, five N-atoms, two O-atoms and 4 benzene rings which contain π -electrons and (ii) it has larger molecular size. Inhibitor (B) comes after compound (A) in inhibition efficiency this is due to: (i) It has 4-O atoms, 4-N atoms, one-S atom and three benzene rings and (ii) it has lesser molecular size than compound (A). Compound (C) is the least effective one due to: (i) It has 2-O atoms, 5-N atoms, one-S atom and three benzene rings and (ii) it has lesser molecular size than compounds A & B.

Conclusions

- 1) The tested Pyridopyrimidine derivatives establish a very good inhibition for C-steel corrosion in HCl solution
- 2) Pyridopyrimidine derivatives inhibit C-steel corrosion by adsorption on its surface and act better than the passive oxide film
- 3) The inhibition efficiency is in accordance to the order: $A > B > C$
- 4) The inhibition efficiencies of the tested compounds increase with increasing of their concentrations
- 5) Double layer capacitances decrease with respect to blank solution when the inhibitor added. This fact may explained by adsorption of the inhibitor molecule on the C-steel surface
- 6) The adsorption of these compounds on C-steel surface in HCl solution follows Temkin adsorption isotherm
- 7) The values of inhibition efficiencies obtained from the different independent techniques used showed the validity of the obtained results

References

- [1] G. TrabANELLI, inhibitors - an old remedy for a new challenge Corrosion 47 (1991) 410
- [2] D.N. Singh, A.K. Dey, Corrosion 49 (1993) 594
- [3] G. Banerjee, S.N. Malhotra, Corrosion-NACE 48 (1992) 10
- [4] S.T. Arab, E.A. Noor, Corrosion, 49 (1993) 122.

- [5] I.A. Raspini, Corrosion, 49 (1993) 821
- [6] N. Hajjaji, I. Ricco, A. Shiri, A. Lattes, M. Soufiaoui, A. Benbachir, Corrosion, 49 (1993) 326
- [7] M. Elachouri, M.S. Hajji, M. Salem, S. Kertit, R. Coudert, E.M. Essassi, Corros. Sci. 37 (1995) 381
- [8] H. Luo Y.C. Guan, K.N. Han, Corrosion, 54 (1998) 619
- [9] M.A. Migahed, E.M.S. Azzam, A.M. Al-Sabagh, Mater.Chem.Phys. 85 (2004) 273
- [10] M.M. Osman, A.M. Omar, A.M. Al-Sabagh, Mater Chem. Phys. 50 (1997) 271
- [11] F. Zucchi, G. TrabANELLI, G. Brunoro, Corros. Sci. 33 (1992) 1135
- [12] R.F.V. Villamil, P. Corio, J.C. Rubim, M.L. Silva Agostinho, J. Electroanal. Chem. 472 (1999) 112
- [13] T.P. Zhao, G.N. Mu, Corros. Sci. 41 (1999) 1937
- [14] S.S. Abd El Rehim, H. Hassan, M.A. Amin, Mater. Chem. Phys. 70 (2001) 64
- [15] S.S. Abd El Rehim, H. Hassan, M.A. Amin, Mater. Chem. Phys. 78 (2003) 337
- [16] R. Guo, T. Liu, X. Wei, Colloids Surf. A 209 (2002) 37
- [17] V. Branzoi, F. Golgovici, F. Branzoi, Mater. Chem. Phys. 78 (2002) 122
- [18] F. Bentiss Traisnel, M. Lagrenee, Corros. Sci. 42 (2000) 127
- [19] M.A.B. Christopher, A.R.G. Isabel Jenny, Corros. Sci. 36 (1994) 915
- [20] M. Elachouri, M.S. Hajji, M. Salem, S. Kertit, J. Aride, R. Coudert, E. Essassi, Corrosion, 52 (1996) 103
- [21] A.S. Algaber, E.M. El-Nemma, M.M. Saleh, Mater. Chem. Phys. 86 (2004) 26
- [22] G.N. Mu, T.P. Zhao, M. Liu, T. Gu, Corrosion 52 (1996) 853
- [23] R.G. Parr, D.A. Donnelly, M. Levy, M. Palke, J. Chem. Phys. 68 (1978) 3801
- [24] A.K. Maayta, N.A.F. Al-Rawashdeh, Corros. Sci. 46 (2004) 1129
- [25] J. Aljourani, K. Raeissi, M.A. Golozar, Corros. Sci., 51 (2009) 1836
- [26] H. Amar, A. Tounsi, A. Makayssi, A. Derja, J. Benzakour, A. Outzourhit, Corros. Sci. 49 (2007) 2936
- [27] M.A. Migahed, E.M.S. Azzam, S.M.I. Morsy, E Corros. Sci. 51 (2009) 1636
- [28] M.N.H. Moussa, A.A. El-Far, A.A. El-Shafei, Mater. Chem.Phys. 105 (2007) 105
- [29] M. Benabdellah, R. Touzan, A. Aouniti, A.S. Dafali, S. El-Kadiri, B. Hommouti, M. Benkaddour, Mater. Chem. Phys. 105 (2007) 373
- [30] E. Bayol, K. Kayakirilmaz, M. Erbil, Mater. Chem. Phys. 104 (2007) 74
- [31] O. Benalli, L. Larabi, M. Traisnel, L. Gengembra, Y. Harek, Appl. Surf. Sci. 253 (2007) 6130

- [32] I. Epelboin, M. Keddam, H. Takenouti, J. Appl. Electrochem. 2 (1972) 71-79
- [33] J. C. Bessone Mayer, K. Tuttner, W.J. Lorenz, Electrochim. Acta 28 (1983) 171-172
- [34] E.A. Noor, A.H. Al-Moubaraki, Mater. Chem. Phys. 145 (2008) 110
- [35] G. Moretti, G. Quartanone, A. Tassan, A. Zingales, Wekst. Korros. 45 (1994) 641
- [36] H. Ashassi-Sorkhabi, N. Ghalebsaz-Jeddi, Mater. Chem. Phys. 92 (2005) 480
- [37] E. Khamis, Corrosion (NACE) 46 (1990) 476
- [38] A.A. El-Awady, B. Abd El-Nabey, S.G. Aziz Electrochem. Soc. (1992) 139 2149
- [39] J. Lipkowski, P.N. Ross (Eds.) Adsorption of Molecules at Metal Electrodes, VCH, New York (1992)
- [40] S.L.F.A., Da Costa, S.M.L. Agostinho, Corros. Sci. 45 (1989) 472
- [41] E.F. El-Sherbiny, Mater. Chem. Phys. 60 (1999) 286
- [42] A.S. Fouda, A.A. Al-Sarawy, E.E. El-Katori, Desalination 201 (2006) 1
- [43] G. Gao, C. Liang, Acta Electrochem (2007) 52 4554
- [44] G. Gece, S. Bilgic Corros. Sci. 51 (2009) 1876
- [45] S. Martinez, Mater. Chem. Phys. 77 (2002) 97
- [46] Ishtiaque Ahamad, Rajendra Prasad, M.A. Quraishi, Corros. Sci. 52 (2010) 3033
- [47] G.N. Mu, T.P. Zhao, M. Liu, T. GU, Corrosion 52 (1996) 83
- [48] Ashish Kumar Singh, M.A. Quraishi, Corros. Sci. 52 (2010) 1529

الملخص العربي

تنشيط تأكل الصلب الكربوني في حمض الهيدروكلوريك باستخدام مشتقات البريدوبريميدين

عبد العزيز فودة¹، مصطفى دياب²، أشرف البنداري²، أحمد أبو بكر¹

¹ قسم الكيمياء – كلية العلوم – جامعة المنصورة

² قسم الكيمياء – كلية العلوم – جامعة دمياط

تم دراسة تنشيط تأكل الصلب الكربوني في 0.5 مولر حمض الهيدروكلوريك باستخدام بعض مشتقات البريدوبريميدين وذلك بطريقتي الفقد في الوزن والاستقطاب البوتنشيو ديناميكي عند درجات حرارة مختلفة وطريقتي المعاوقة الكهربائية عند درجة حرارة 25°م وكذلك دراسة السطح بواسطة المجهر الإلكتروني والتحليل الطيفي للتشتت الطاقة. وقد وجد أن كفاءة التنشيط تعتمد على نوع المثبط وكذلك تركيزه وأن كفاءة التنشيط تقل بارتفاع درجة الحرارة. وجد أن هذه المشتقات تمتص على سطح الصلب الكربوني تابعة لآيزوثرم تمكّن. وقد وجد أن سعة الطبقة الكهربائية المزدوجة تقل مع التركيز ومقاومة انتقال الشحن تزداد. تم حساب ومناقشة بعض الدوال الترموديناميكية لعملية التآكل. وجد أن كفاءة التنشيط تعتمد على المجموعات المعطية في المركب. تم ترتيب المثبطات تبعا لكفاءتها لعملية التنشيط.